



MODELING THE SPATIALLY VARYING WATER BALANCE PROCESSES IN A SEMIARID MOUNTAINOUS WATERSHED OF IDAHO¹

Benjamin T. Stratton, Venkataramana Sridhar, Molly M. Gribb,
James P. McNamara, and Balaji Narasimhan²

ABSTRACT: The distributed Soil Water Assessment Tool (SWAT) hydrologic model was applied to a research watershed, the Dry Creek Experimental Watershed, near Boise Idaho to investigate its water balance components both temporally and spatially. Calibrating and validating SWAT is necessary to enable our understanding of the water balance components in this semiarid watershed. Daily streamflow data from four streamflow gages were used for calibration and validation of the model. Monthly estimates of streamflow during the calibration phase by SWAT produced satisfactory results with a Nash Sutcliffe coefficient of model efficiency 0.79. Since it is a continuous simulation model, as opposed to an event-based model, it demonstrated the limited ability in capturing both streamflow and soil moisture for selected rain-on-snow (ROS) events during the validation period between 2005 and 2007. Especially, soil moisture was generally underestimated compared with observations from two monitoring pits. However, our implementation of SWAT showed that seasonal and annual water balance partitioning of precipitation into evapotranspiration, streamflow, soil moisture, and drainage was not only possible but closely followed the trends of a typical semiarid watershed in the intermountain west. This study highlights the necessity for better techniques to precisely identify and drive the model with commonly observed climatic inversion-related snowmelt or ROS weather events. Estimation of key parameters pertaining to soil (e.g., available water content and saturated hydraulic conductivity), snow (e.g., lapse rates, melting), and vegetation (e.g., leaf area index and maximum canopy index) using additional field observations in the watershed is critical for better prediction.

(KEY TERMS: hydrologic cycle; streamflow; evapotranspiration; vadose zone; SWAT model; Idaho.)

Stratton, Benjamin T., Venkataramana Sridhar, Molly M. Gribb, James P. McNamara, and Balaji Narasimhan, 2009. Modeling the Spatially Varying Water Balance Processes in a Semiarid Mountainous Watershed of Idaho. *Journal of the American Water Resources Association* (JAWRA) 45(6):1390-1408. DOI: 10.1111/j.1752-1688.2009.00371.x

INTRODUCTION

The need to better understand the hydrologic characteristics of snow-dominated semiarid water-

sheds at the regional scale of the inland Northwest is heightened by a near doubling of the region's population since 1970 (Rudзитis and Johnson, 2000). This rapid population growth is expected to impact the function of the watersheds of the region through

¹Paper No. JAWRA-09-0005-P of the *Journal of the American Water Resources Association* (JAWRA). Received January 13, 2009; accepted August 12, 2009. © 2009 American Water Resources Association. **Discussions are open until six months from print publication.**

²Respectively Hydrologist (Stratton), GMUG National Forests SO, Delta, Colorado; Assistant Professor and Professor (Sridhar and Gribb), Department of Civil Engineering, Boise State University, Boise, Idaho 83725; Professor (McNamara), Department of Geosciences, Boise State University, Boise, Idaho 83725; Assistant Professor (Narasimhan), Department of Civil Engineering, Indian Institute of Technology, Chennai, India (E-Mail/Sridhar: vsridhar@boisestate.edu).

activities such as land management, dam building, and timber harvesting (Bales *et al.*, 2006; Mote *et al.*, 2003). Since it is difficult to obtain continuous direct measurements with sufficient spatial coverage in mountain ecosystems, a robust computational hydrologic model that simulates fluxes of energy and water between the atmosphere and the land surface can be an effective means of studying land-surface dynamics. Hydrologic models with complex soil-vegetation schemes can also be useful to extrapolate estimates of land surface fluxes beyond the resolution of point measurements, provided the land surface characteristics are properly represented in the model. Such models are capable, after robust evaluation, of providing continuous predictions of the components of the water balance with a high degree of confidence across a range of ecosystems and climate divisions.

Various water balance components and their roles in controlling carbon cycling, energy flux, and other biogeochemical processes have been studied extensively. These significant water balance components include: soil moisture storage (Li and Islam, 2002; Sridhar *et al.*, 2006), evapotranspiration (ET) (Flerchinger *et al.*, 1996; Narasimhan *et al.*, 2005; Ryu *et al.*, 2008; Sun *et al.*, 2008), streamflow generation, and soil drainage (Grant *et al.*, 2004; Schüttmeyer *et al.*, 2006). Large-scale hydrologic models have successfully been used to estimate soil moisture in many mesoscale efforts (e.g., Huang *et al.*, 1996; Houser *et al.*, 1998; Entin *et al.*, 1999). These previous studies were conducted at river basin to continental scales, primarily in agricultural or grassland areas. Little work, however, has been conducted to estimate the water balance components of streamflow, soil moisture storage, and ET at the catchment scale in topographically complex snow-dominated semiarid catchments.

The snow-dominated mountain catchments in semiarid environments present considerable challenges for spatially distributed modeling due to highly heterogeneous climate drivers, complex topography, and environmental gradients. Since the field monitoring sites are sparse, accurately extrapolating both temperature and precipitation across mountainous terrain is difficult. Therefore, both precipitation and temperature lapse rates computed for this data-limited region can only be an approximation at best and they can limit the ability of the model to capture the watershed processes. Complex topography introduces diverse snowmelt patterns, and large elevation gradients can produce complicated precipitation distributions. For example, a rain-snow elevation transition can occur as a result of a negative temperature lapse rate where higher elevations are below freezing while lower elevations are above freezing. However,

temperature inversions are common to the mountain basin areas during times of stable high pressure winter time conditions. Rain-on-snow (ROS) events common to the Pacific Northwest further complicate the prediction of possible spring time extreme flood events (Marks *et al.*, 1998). Vertical temperature and precipitation gradients produce complex vegetation distributions that complicate streamflow, soil moisture, and ET estimation. Mountain catchments are commonly characterized by thin soils overlying fractured bedrock. Williams *et al.* (2008) showed that the spatial and temporal variability of soil moisture is tightly coupled to the spatial variability of snow. Seasonal variability in soil moisture, and hence ET, play a significant role in the streamflow generation for snowmelt-driven hillslope process dominated topographically complex watersheds (Eckhardt *et al.*, 2002; McNamara *et al.*, 2005). The fate of moisture at the soil bedrock interface is difficult to assess, and deep groundwater is often disconnected from streams for long periods of time. These challenges are compounded by a lack of locations with sufficient spatial and temporal information to calibrate spatially distributed models.

The overall purpose of this modeling effort was to explore the spatio-temporal distribution of the water balance components of a complex snow-melt driven semiarid watershed using the distributed Soil Water Assessment Tool (SWAT) model in a data limited environment. This study focused on modeling the hydrological budget for the Dry Creek Experimental Watershed (DCEW) near Boise, Idaho. The watershed contains three weather stations with vertically distributed soil moisture measurements and seven stream gaging stations in a 27 km² area. Using streamflow data measured at the watershed outlet for a six-year period (2001-2007) and soil moisture measurements at two locations from the watershed for the same time period, the hydrological budget of the DCEW was simulated. The specific objectives of this investigation were as follows: (1) to optimize the values of the parameters of the SWAT model governing streamflow volume and timing through calibration, (2) to compare calibrated model predictions with *in-situ* measurements of both streamflow and soil moisture to investigate the water balance components over a three-year period (2004-2007), and (3) to develop seasonal spatio-temporal estimates of the water balance of the watershed.

A review of the historical development and applications of SWAT was conducted by Gassman *et al.* (2007). SWAT has been implemented to adequately estimate streamflow volumes and timing from mountainous watersheds (Eckhardt *et al.*, 2002; Fontaine *et al.*, 2002; Fohrer *et al.*, 2005; Wang and Melesse, 2006; Abbaspour *et al.*, 2007; Lemonds and McCray,

2007; Ahl *et al.*, 2008; Zhang *et al.*, 2008), but little work has been conducted that use these water balance predictions to investigate soil moisture in a spatio-temporal manner. Furthermore, these studies used a simplified scheme for infiltration. All previous applications of SWAT in mountain watersheds have used the Soil Conservation Service curve number (SCS-CN) approach (SCS, 1972) to estimate the infiltration of incoming precipitation. Garen and Moore (2005) suggested that application of the SCS-CN method to predict infiltration is a misuse of the method since it was designed to predict streamflow based on the assumption that all streamflow is the result of overland flow. This assumption is not appropriate for the highly permeable and coarse-textured soils of the DCEW. The Green-Ampt Mein-Larson excess rainfall method (Mein and Larson, 1973), an improved Green and Ampt (1911) infiltration model, referred to as GAML hereafter, is generally well-suited for any soil, and as such, should better represent the layer-wise soil moisture distribution across the watershed.

The work of this study differs from previous studies conducted in mountain watersheds (Hernandez *et al.*, 2000; Fontaine *et al.*, 2002; Lemonds and McCray, 2007; Ahl *et al.*, 2008) in two respects: firstly, the model is applied in a semiarid, snow-dominated environment, and secondly, long-term soil moisture observations, in addition to streamflow measurements, are used to analyze the model biases by

placing equal importance on infiltration and soil moisture initialization. Application of soil moisture data in the water balance assessment of this mountainous environment enhanced the model evaluation substantially. Through calibration and validation of the SWAT model using the GAML infiltration model, this study is expected to provide a better understanding of the spatio-temporal distribution of soil moisture and other water balance components for a mountainous watershed.

MATERIALS AND METHODS

The Dry Creek Experimental Watershed

The DCEW is located in the rolling foothills approximately 8 km north of Boise, Idaho (Figure 1). The outlet of this watershed is located at 43.69°N, 116.18°W North American Datum of 1983 (NAD 83). The land is mainly privately owned and managed (54.7% of the watershed by area) while the remainder of the watershed is managed as public lands (42.9% by the United States Forest Service and 2.4% by the State of Idaho). Dry Creek is a perennial stream that runs in a southwesterly direction eventually draining into the Boise River. Dry Creek has one perennial named tributary, Shingle Creek, with a drainage area

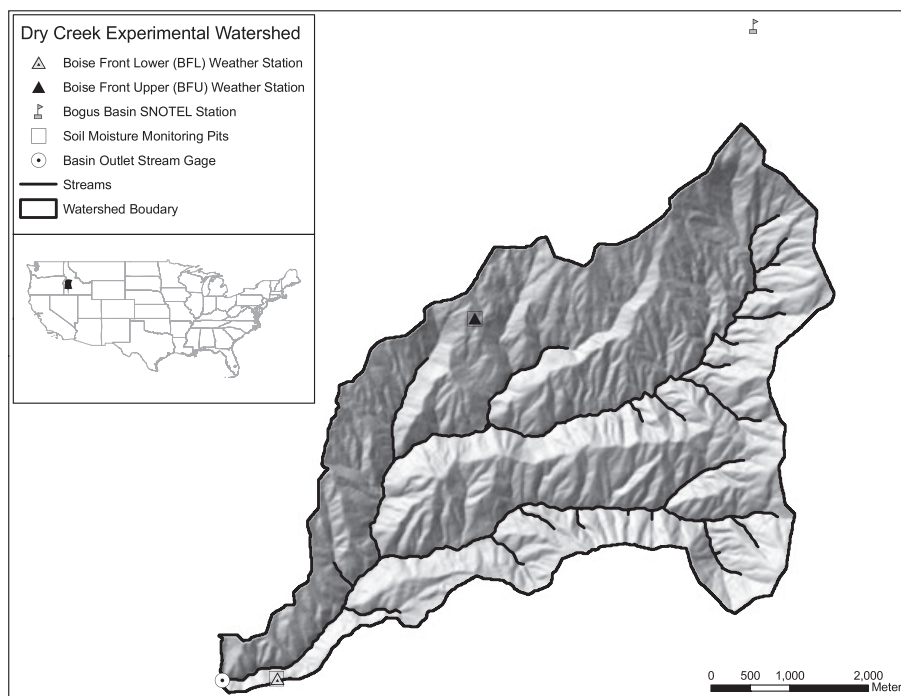


FIGURE 1. Dry Creek Experimental Watershed Location Map.

of 8.6 km² and many smaller unnamed intermittent and ephemeral tributaries.

The DCEW's elevation ranges from 1,033 m at the basin outlet, captured by the lowest stream gage, to 2,133 m at the headwater ridge of the basin. Land cover of the watershed varies greatly with elevation and aspect. The lower (or desert) tree line elevation, the lowest and driest elevation at which trees can grow, varies with hillslope aspect from as low as 1,300 m on north facing slopes to as high as 1,650 m on south facing slopes. The vegetation in the catchment can best be described as shrub steppe and grasslands below tree line, and mixed conifer forest above tree line (Caicco *et al.*, 1995). Soils throughout the watershed display a high level of spatial variability as a function of elevation and aspect (Natural Resources Conservation Service, United States Department of Agriculture, 2005). Based on the USDA NRCS Soil Survey Geographic (SSURGO) database, the soils are generally shallow and well drained with an average depth to bedrock of 1.2 m and an average saturated hydraulic conductivity in the range of 10.15-610.11 mm/h.

Temporal soil moisture patterns reflect the hydrologic seasonality of the catchment. Soil moisture conditions exhibit prolonged, stable summertime dry periods and wintertime wet periods separated by dynamic transition periods in fall and spring. This seasonality creates complex runoff generation scenarios, i.e., similar storms during dry and wet periods produce very different responses. Rain during the summer is generally consumed by evaporation from

soil and vegetation surfaces, whereas rain during wet periods can contribute to streamflow. Using a chloride mass balance approach, Aishlin (2006) showed that considerable amounts of water infiltrates into the bedrock at higher elevations, but that at the large catchment scale losses to deep groundwater are negligible, meaning that bedrock infiltration in the high elevations re-emerges as springs and stream base flow.

Micrometeorological Measurements

Two of the watershed's three weather stations were used for this work: the Boise Front Lower (BFL) and Boise Front Upper (BFU) stations (Figure 1). The BFL station is located at 43.69°N, 116.17°W (NAD 83) at an elevation of 1,151 m while the upper station, BFU, is located in the Treeline Catchment at 43.73°N, 116.14°W (NAD 83) at an elevation of 1,612 m. The third station, Lower Deer Point, has only been online since 2006 and does not yet have data records that are long enough to be useful to these modeling efforts. The outlet stream gage of the DCEW is used to best demonstrate the catchment-scale streamflow predictive abilities of SWAT.

The basin generally has cold wet winters and hot dry summers with occasional localized rainstorms. Daily average temperatures from December to February are approximately 0°C with a monthly average of 68 mm of precipitation, while the June to August daily average temperatures are 22°C with a monthly average of 7 mm of precipitation (Figure 2). Based on

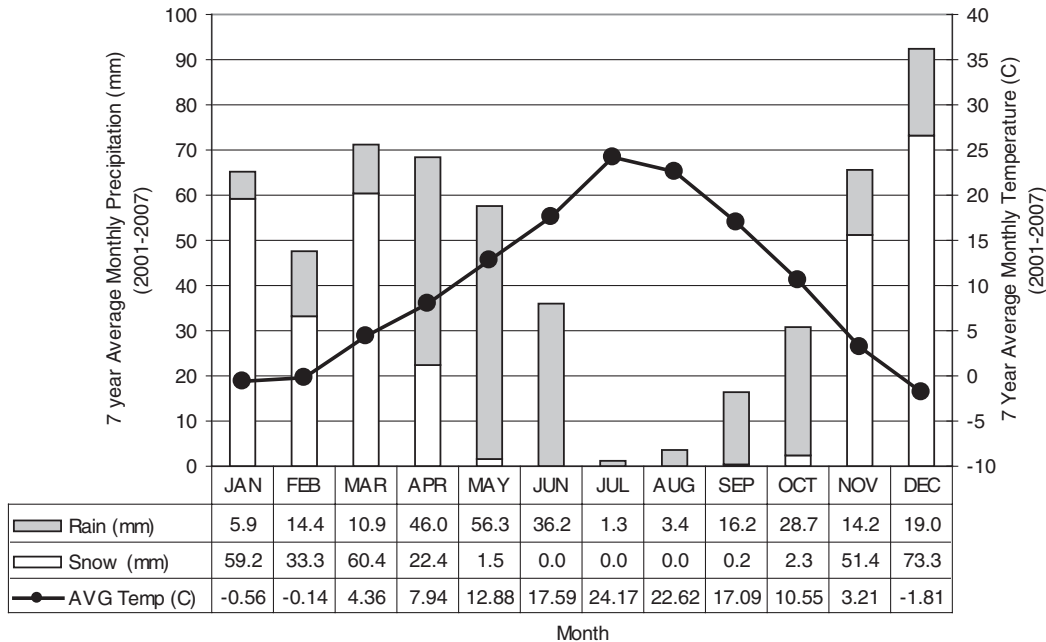


FIGURE 2. DCEW Seven Year Average Monthly Precipitation and Temperature (2001-2007).

hydroclimatological analysis conducted for this work, about 54% of the precipitation that falls on the basin comes in the form of snow. The Koppen classification of the lower elevations of the basin is steppe summer dry climate (BsK) while the upper elevation is moist continental climate with dry summers (Dsa) (McNamara *et al.*, 2005).

SWAT Model Description

SWAT is a continuous simulation macroscale hydrologic model that operates on a daily time step and is designed to predict the impacts of land management on the water yield of large ungaged watersheds (Santhi *et al.*, 2001). SWAT provides physically based algorithms as an option to describe many of the important components of the hydrologic cycle. The input requirements of the model are data describing a basin's weather, soil properties, topography, vegetation, and land management practices. Since SWAT is a continuous time, or long-term yield model, as opposed to a single event storm simulator, it is better suited for simulating a watershed's seasonal or yearly fluctuations of water balance components rather than predicting single event flood routing (Sun and Cornish, 2005). The most current version of the model, SWAT2005 (herein referred to as SWAT), was used in this work with ArcSWAT, a GUI developed by Olivera *et al.* (2006) that works as an extension within the Environmental Systems Research Institute (ESRI) GIS software package ArcMAP (ESRI, Redlands, California). A detailed description of the model and its applications can be found elsewhere (Arnold *et al.*, 1998; Srinivasan *et al.*, 1998; Neitsch *et al.*, 2005; Arnold and Fohrer, 2005; Jayakrishnan *et al.*, 2005).

SWAT can be broken into two major components: a land phase, and a routing phase. The land phase of the model distributes the incoming precipitation between the possible hydrologic pathways (all units are mm per unit area) through the water balance equation:

$$SW_t = SW_0 + \sum_{i=1}^t (R_{\text{day}} - Q_{\text{surf}} - E_a - w_{\text{seep}} - Q_{\text{gw}}), \quad (1)$$

where SW_t is the final soil water content on day i , SW_0 is the initial soil water content during time step i , t is the time step (hours, days, or months), R_{day} is the amount of precipitation during time step i , Q_{surf} is the amount of surface runoff on time step i , E_a is the amount of ET during time step i , w_{seep} is the amount of water entering the vadose zone during

time step i , and Q_{gw} is the amount of deep drainage that contributes to groundwater recharge during time step i (Neitsch *et al.*, 2005).

The second major component of the SWAT model, that covers the flow through channels and reservoirs, is the routing phase. Here algorithms route water through the main channels of the watershed using either a variable storage coefficient method developed by Williams (1969), or the Muskingum routing method (Neitsch *et al.*, 2005).

Snowmelt Formulation. Snowmelt within the SWAT model is governed by a temperature index method controlled by air temperature, snowpack temperature, melt rate, and a measure of the areal coverage of snow (Fontaine *et al.*, 2002; Neitsch *et al.*, 2005). The snowmelt depletion modifications implemented by Fontaine *et al.* (2002) yielded much more useful predictions of the mountain watershed's response to precipitation and melt events than the unmodified SWAT model and this scheme is now a part of the SWAT2005 code that was used in this investigation. The most significant changes they made included the integration of algorithms that utilize elevation bands to distribute both snow accumulation and melt, and a new accounting procedure for correcting simulated losses in snow water equivalent (SWE) as the fractional snow-covered area (SCA) is reduced. The SWE-SCA relationship is defined within the model by an areal snow coverage depletion curve. This curve is defined by the SWE value for 50% areal extent snow cover (SNOCOV50), the origin, and a point of total coverage defined as maximum snow cover at 95% snow cover (SNOCOVMAX) and 95% of maximum SWE. The shape of the depletion curve defines the incremental melt-water released as a function of changes in areal snow cover of the basin. The depletion curve is used to correct the volume of predicted meltwater outputs for the proportion of the modeled area that is partially covered with snow. This curve compensates for the heterogeneous nature of snow distribution throughout a basin as a result of differential accumulation and melt.

Model Implementation

Weather Station Data. Weather data to drive the SWAT model, as well as layer-wise soil moisture data for use in calibration and validation of the model, were collected at two meteorological stations within the DCEW. Two primary weather stations, BFU and BFL, provide the weather variables needed for SWAT: incoming long wave solar radiation (MJ/m^2), daily maximum and minimum temperature ($^{\circ}\text{C}$), daily average wind speed (m/s), daily average

relative humidity (%), and hourly precipitation (mm). Noise in the precipitation measurements characteristic of weighing-bucket gages was eliminated using a precipitation correction algorithm (Nayak *et al.*, 2008). Both stations provide soil moisture data at multiple depths in two adjacent pits at each location. Soil moisture data are measured and recorded in both pits, at both locations, at 15-min intervals with Campbell Scientific, CS-615, water content reflectometers (WCR) (Campbell Scientific, Logan, Utah) at depths of 15, 30, 60, and 100 cm. These WCR moisture content measurements have been calibrated to time domain reflectometry probes to an accuracy of $\pm 2\%$ (Chandler *et al.*, 2004).

Continuous records of hourly precipitation data are inputs for the SWAT GAML infiltration submodel. However, due to power supply issues and/or instrument malfunction, both stations have experienced week- to month-long data gaps and these were filled by incorporating data from a third weather station maintained by the NRCS SNOTEL located 5.1 km to the northeast of the BFU station at the Bogus Basin ski area, 43.76°N, 116.10°W (NAD 83) 1,932 m elevation (Figure 1). Hourly precipitation data from the Bogus Basin SNOTEL site (BB) (NRCS SNOTEL, 2007) were used with monthly precipitation ratios developed from the entire period of record for the three weather stations. The gap-filled precipitation data were subsequently used to simulate precipitation events during periods of data logger failure in an event-by-event manner. For example, during a

gap, if a 1-h, 10-mm precipitation event was measured at the BB site and the ratio of monthly average precipitation for that month between the BFL and BB site was 0.80, then an 8-mm event was assigned to the BFL site for that same time period. These corrections were carried out in a manner that preserved the volume of precipitation, as well as its timing and intensity.

Land Surface Description. The SWAT model relies on discretization of unique hydrologic response units (HRUs) that are defined by unique combinations of categorized land covers, soil types, and slope, rather than a predefined grid matrix. It is important to note that the spatial structure of features in SWAT can only be prescribed at the subwatershed level. Therefore, in order to capture the impact of spatially explicit processes at the watershed outlet, the basin must be subdivided in a way that reflects in complexity. While some spatial detail can be incorporated with elevation and slope bands, HRU values are, however, aggregated over subwatersheds and discretization of subwatersheds clearly determines the representation of subgrid scale spatial variability. Discretization of HRUs is accomplished using the ArcSWAT GUI (Olivera *et al.*, 2006). The GUI relies on readily available national datasets that consist of a digital elevation model (DEM) grid, vegetation map, and a soils map. As shown in Figure 3, the DCEW was subdivided into five subbasins made up of 839 unique HRUs that have average areas of 0.03 km².

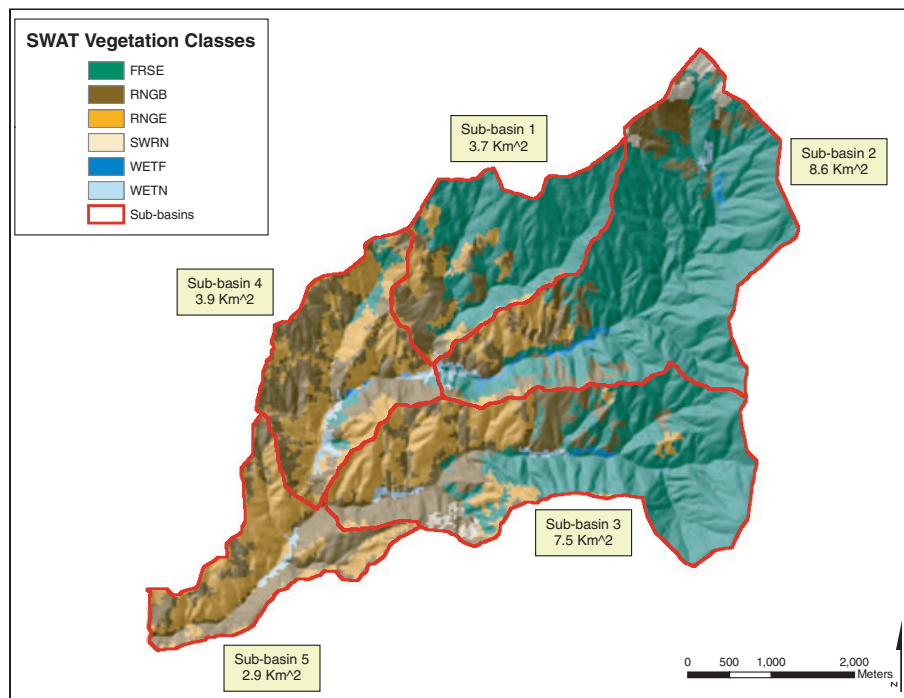


FIGURE 3. DCEW Subbasins Delineated to Match Resolution of Stream Gage Network and SWAT Land Use Classification.

A 10×10 m horizontal scale DEM obtained from the National Elevation Dataset (NED) (Idaho Geospatial Data Clearinghouse, 2004) was used in this study. The hillslopes of the basin were discretized into five slope classes, which is the maximum number allowed by ArcSWAT. Slope class divisions were set at quantile points so each class represents 20% of the basin area. These elevation data were also used to delineate the DCEW into 100-m elevation bands to drive the distribution of temperature and precipitation data as described by Fontaine *et al.* (2002).

Remotely sensed LANDSAT images processed for the GAP (Gap Analysis Program) Analysis of Idaho were used to describe the vegetation of the DCEW (Caicco *et al.*, 1995; Landscape Dynamics Lab, 1999) at a 30×30 m horizontal resolution. The Idaho GAP analysis delineated the DCEW into 18 different vegetation types. These vegetation types were remapped to match six SWAT model vegetation types (Table 1 and Figure 3). Forested evergreen (FRSE) covers 49% of the watershed's area, making it the dominant land cover. Rangeland brush (RNGB) and range grass (RNGE) nearly make up the remaining area of the watershed (47%).

The USDA NRCS SSURGO database (Natural Resources Conservation Service, United States Department of Agriculture, 2005) was used to characterize the geospatial extents and physical properties of 28 different soil types across the DCEW. The county-level SSURGO soils coverage was chosen over the lower-resolution State Soil Geographic Database (STATSGO) (Natural Resources Conservation Service, United States Department of Agriculture, 2006). In the case of the DCEW, the SSURGO coverage provides a finer resolution description of the soils; SSURGO delineates 28 soils while STATSGO shows two soil types.

Soils were classified according to the USDA classification system (Soil Survey Staff, 1975) as gravelly sand and sand in the vicinity of the BFU measurement location, and loam approaching sandy-loam at the BFL site. Undisturbed core soil samples from

multiple locations and depths in a small catchment near the BFU were subjected to laboratory falling head tests to obtain an average saturated conductivity value of 133 mm/h, which compares well to the values provided by the SSURGO database (Gribb *et al.*, 2009).

Model Parameterization. Following the work of Fontaine *et al.* (2002), the parameters related to lapse rates reflecting the DCEW characteristics were fixed to match observed values from four weather stations; the three described in the previous section: BFL, BFU, and the BB, and a lower elevation site located at the Boise Airport maintained by the National Oceanic and Atmospheric Association National Weather Service (NOAA NWS). The Boise Airport (BOI) site is located 13.9 km south of the DCEW outlet, 43.62°N , 116.22°W (NAD 83) at an elevation of 825 m. Eight years (2000-2007) of data from the BOI, BFL, and BFU stations were analyzed to arrive at a temperature lapse rate as a function of elevation (dT/dz). The yearly average temperature lapse rate for these three stations is $-3.2^\circ\text{C}/\text{km}$ ($R^2 = 0.91$). Similarly, an average precipitation lapse rate (dP/dz) of 462.9 mm/km ($R^2 = 0.74$) was computed by analysis of eight years of yearly average precipitation (2000-2007) from the BFL, BFU, and BB stations.

Parameter Sensitivity Analysis. Sensitivity analysis techniques allow a better understanding of the relative importance of the model parameters, and aid in identifying the parameters to which the model is most sensitive. In this work, a Latin hypercube one-at-a-time (LH-OAT) method is used to assess SWAT's sensitivity to parameters specific to the DCEW to provide direction during the calibration-phase of the model set up. The LH-OAT method developed by van Griensven *et al.* (2006) discretizes the parameter space into a number of units and then systematically varies from random seed numbers within these units to more effectively sample the domain. The LH-OAT method was used to evaluate the relative sensitivity of the 27 flow parameters considered in this study (Table 2) and to rank them by varying them over defined ranges and comparing the changes in model streamflow predictions. These 27 parameters include the snow-related parameters that were found to be important in the work of earlier research: snowpack temperature lag factor (TIMP), maximum snowmelt factor (SMFMX), minimum snowmelt factor (SMFMN), areal snow coverage threshold (SNOCOCMX), threshold snowfall temperature (SMTMP), and threshold snow formation temperature (SFTMP) (Lemonds and McCray, 2007).

Upon evaluation of the LH-OAT sensitivity analysis ranking, 11 of the most sensitive parameters were

TABLE 1. Summary of SWAT Land Description Classes for DCEW.

SWAT Vegetation Class	Area of DCEW (%)
SWRN	1.2
RNGE	22.5
RNGB	24.9
FRSE	49.2
WETF	0.7
WETN	1.5

Notes: FRSE, Forested Evergreen; RNGB, Rangeland Brush; RNGE, Rangeland Grass; SWRN, Southwestern Range Land; WETF, Wetland Forested; WETN, Wetland Nonforested.

TABLE 2. SWAT Flow Parameters Considered for Sensitivity Analysis.

Parameter	Description
ALPHA_BF	Base flow alpha factor (days)
BIOMIX	Biological missing efficiency (unitless)
BLAI	Leaf area index (unitless)
CANMX	Maximum canopy index (mm)
CH_K2	Effective channel hydraulic conductivity (mm/h)
CH_N	Manning coefficient for channel (unitless)
CN2	SCS-CN for moisture condition II (unitless)
EPCO	Plant evaporation compensation factor (unitless)
ESCO	Soil evaporation compensation factor (unitless)
GW_DELAY	Groundwater delay (days)
GW_REVAP	Groundwater reevaporation coefficient (unitless)
GWQMN	Threshold depth of water in the shallow aquifer required for return flow to occur (mm)
RCHRG_DP	Groundwater recharge to deep aquifer (fraction)
REVAPMIN	Threshold depth of water in the shallow aquifer for reevaporation to occur (mm)
SFTMP	Snowfall temperature (°C)
SLOPE	Average slope steepness (m/m)
SLSUBBSN	Average slope length (m)
SMFMN	Minimum melt rate for snow during the year (mm/°C/day)
SMFMX	Maximum snowmelt rate (mm/°C/day)
SMTMP	Snowmelt base temperature (°C)
SOL_ALB	Soil albedo
SOL_AWC	Available water capacity of the soil layer (mm/mm)
SOL_K	Soil conductivity (mm/h)
SOL_Z	Soil depth (mm)
SURLAG	Surface runoff lag coefficient
TIMP	Snowpack temperature lag factor
TLPAS	Temperature lapse rate (°C/km)

selected for model autocalibration (Table 3). Parameters that the model was very sensitive to, but reasonably accurate values were readily available for (such as soil depth and hillslope from the DEM analysis) were not included in the autocalibration. The 11 parameters identified in the sensitivity analysis also

represented the parameters that could not be easily measured or estimated for the basin and for which realistic default values were not available due to lack of information, such as the leaf area index (BLAI), maximum canopy index (CANMX), and plant evaporation compensation factor (EPCO). However, some parameters with adequate estimates provided by input databases, such as saturated soil conductivity (SOL_K) and soil available water content (SOL_AWC) were included in the autocalibration because the sensitivity analysis showed that they are significantly controlling the model's predictive powers, and due to poor uncalibrated model predictions, needed adjustment.

Model Calibration. Calibration of the SWAT model was necessary as the model is composed of a large number of parameters that define various watershed characteristics and flow processes that are not accurately characterized by default input parameters or easily measured in the field. This calibration was aimed at obtaining a Nash Sutcliffe coefficient of efficiency (NSE) value of at least 0.75 for the generated daily stream discharge predictions thereby eventually matching observed discharge volumes and timing. Automation of the calibration procedure for the parameters identified in the sensitivity analysis was done using the shuffled complex evolution method developed at the University of Arizona (SCE-UA). The SCE-UA method developed by Duan *et al.* (1992, 1994) is integrated into the ArcSWAT GUI. This autocalibration method varies user-defined parameters within prescribed ranges to arrive at a parameter set that best simulates the observed discharge for a calibration period, based on minimization of an objective function. This method has worked well for autocalibration of the SWAT model in a variety of watersheds around the world (e.g., Duan *et al.*, 1994; Eckhardt *et al.*, 2002; White and Chaubey,

TABLE 3. Sensitive Parameters Chosen for Model Calibration, Calibration Range, Default Values, and Calibrated Parameter Value (calibration values that are reported as percentages represent the percentage change from the initial value of the parameter).

Parameter	SWAT Parameter	Default Value	Calibration Range	Optimized Value
Base flow alpha factor (days)	ALPHA_BF	0	0-1	0.60
Leaf area index (unitless)	BLAI	Varies by vegetation	-50 to 50%	15.23%
Maximum canopy index (mm)	CANMX	0	0-10	8.62
Plant evaporation compensation factor (unitless)	EPCO	0	0-1	0.57
Soil evaporation compensation factor (unitless)	ESCO	0	0-1	0.61
Groundwater recharge to deep aquifer (fraction)	RCHRG_DP	0.05	0-1	0.99
Threshold depth of water in the shallow aquifer for reevaporation to occur (mm)	REVAPMIN	1	0-100	62.85
Snowmelt base temperature (°C)	SMTMP	0.5	0-5	3.03
Available water capacity of the soil layer (mm/mm soil)	SOL_AWC	Varies by soil	-95 to 100%	26.33%
Soil saturated hydraulic conductivity (mm/h)	SOL_K	Varies by soil	-100 to +100%	-94.95%
Snowpack temperature lag factor (unitless)	TIMP	1	0-1	0.05

2005). The calibration procedure was carried out at a daily time step to take advantage of the resolution of hourly precipitation data and the GAML infiltration method. Calibration at the daily time step, rather than monthly time step, makes this work different from most calibrations previously conducted in mountain watersheds by other researchers (e.g., Fontaine *et al.*, 2002; Lemonds and McCray, 2007; Zhang *et al.*, 2008). In the modeling context, it is normally recommended to calibrate the model at the same time step as that of the processes that are of interest. For instance, if soil moisture and ET need to be assessed at the daily time step, it is ideal to calibrate the model at the same time step. For the overall water balance assessment at the seasonal scale (monthly), it is necessary and sufficient to calibrate at the monthly time step. The calibration analysis in this study included 5,709 model runs involving 3.5 for each run, and amounting to 14 days.

A split sample technique was used with the seven years (2001-2007) of weather driver data and streamflow observations available from the DCEW outlet gaging station to calibrate and validate the model performance and system behavior. Calibration simulations began with a one-year spin-up period to allow the model to reach an equilibrium state using weather driver data from 2001. Our choice of using one-year as the spin up was constrained by the availability of long-term data. Data from years 2002 to 2004 were then used as a three-year calibration-phase, while years 2005-2007 were used for validation.

Four metrics were used to measure the model streamflow prediction performance with respect to observed values during calibration and validation. These four objective functions were the NSE (Equation 2) (Nash and Sutcliffe, 1970), the sum of squared errors (SSQ) (Equation 3), volumetric efficiency (VE) (Criss and Winston, 2008) (Equation 4) and deviation in total volume (Dv) (Equation 5) (ASCE, 1993). The corresponding equations are:

$$NSE = 1 - \frac{\sum (O - P)^2}{\sum (O - \bar{O})^2} \tag{2}$$

$$SSQ = \sum (O - P)^2 \tag{3}$$

$$VE = 1 - \frac{\sum |P - O|}{\sum O} \tag{4}$$

$$Dv = \frac{V_o - V_p}{V_o} \times 100, \tag{5}$$

where O is the observed streamflow (m^3/s), P is the model-predicted streamflow (m^3/s) and \bar{O} is the

long-term average of observed streamflows (m^3/s). In Equation (5), V_o is the total observed volume of runoff for the modeling time period and V_p is the total predicted volume of runoff for the same time period (both in m^3). NSE and VE (both unitless) values range from $-\infty$ to 1. A NSE value of 1 indicates there is perfect agreement of model predictions to observations, while a value of 0 indicates that \bar{O} is as accurate of a predictor of streamflow as the model estimates, and negative values indicate that \bar{O} is a better estimate of streamflow than the model prediction. VE, as proposed by Criss and Winston (2008), addresses the fact that NSE (Equation 2) overemphasizes large flows by squaring the deviations (McCuen *et al.*, 2006). The VE measures a model's performance of capturing discharge volumes, addressing another limitation of the NSE. Dv (%) is another measure of the ability of the model to capture total volume of runoff. Dv varies from $-\infty$ to $+\infty$ with a value of 0% for a perfect model fit, and smaller magnitude percentages representing better volume prediction than larger percentages (ASCE, 1993).

The automated SCE-UA technique optimizes the SSQ value, a measure of the total magnitude of error for all observations. In addition to the automatic optimization of the SSQ, the NSE, VE, and Dv values were manually monitored to better quantify the model's performance along with the standard statistical metrics of the Coefficient of Determination (R^2) and root mean squared error (RMSE). Table 4 reports the final calibrated values for the 11 parameters that were selected through the sensitivity analysis and adjusted via autocalibration. Of these parameters, three were manually calibrated to a narrow range at first and let the model to autocalibrate to values within 5% of the limits of their specified ranges initially: groundwater recharge to the deep aquifer (RCHRG_DP), saturated hydraulic conductivity (SOL_K), and snowpack temperature lag factor (TIMP). The remaining eight parameters were adjusted through the autocalibration process to a final value that varied significantly from the default values, suggesting that the set of parameters reached

TABLE 4. Summary of SWAT Model Validation Phase (2005-2007) Streamflow Prediction Performance at Five Stream Gaging Stations.

Subbasin	Drainage Area (km^2)	Avg. Obs. Q	NSE	Dv (%)	Ve	RMSE	R^2
1	3.7	0.01	-0.30	346.7	-0.14	0.53	0.47
2	8.6	0.09	0.30	-41.7	0.42	3.94	0.61
3	7.5	0.05	0.36	-15.5	0.30	2.15	0.62
4	16.2	0.08	0.48	22.1	0.42	3.10	0.76
5	26.6	0.15	0.54	-18.9	0.37	7.34	0.76

a globally optimized value as opposed to having followed the default values or having been maximized or minimized to the limits of their range.

RESULTS

Streamflow

In general, seasonal patterns of the water balance components over large areas are relatively stable year to year. The DCEW receives most of its precipitation in the winter months, ranging between 48 and 92 mm per month between November and May. High elevation precipitation is stored as spatially heterogeneous snowpack, and then runs off during

the spring snowmelt as the daytime air temperatures in the basin rise above freezing in March. Lower elevations experience intermittent rain and snowmelt events throughout the winter. The average total monthly precipitation between June and October is generally less than 20 mm (Figure 2). This seasonal trend in precipitation is also apparent in the observed streamflow (Figures 4 and 5) with peak flows occurring in April, base flows dominating for the remainder of the year, and intermittent runoff events in response to ephemeral summer thunderstorms. This section reports the results of the sensitivity analysis and the impacts of the calibration of the sensitive parameters.

Figure 4 shows the daily values for the three-year hydrologic simulation at the basin outlet stream gage for the calibrated model over the calibration time period (January 2002-December 2004). Visual inspection

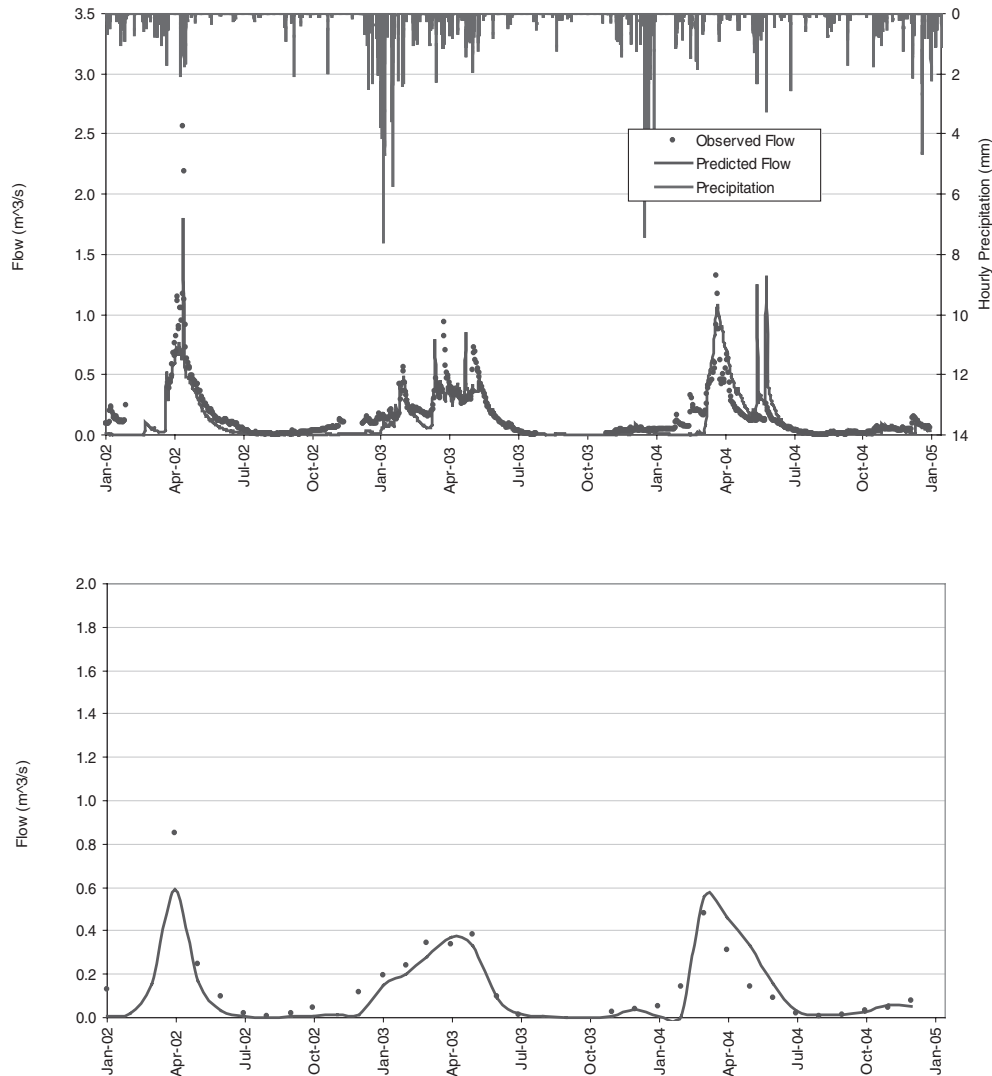


FIGURE 4. Plot of Daily Precipitation With SWAT Simulated and Measured Daily (upper panel) and Monthly Streamflow (lower panel) at Basin Outlet Stream Gage of DCEW for the Calibration Time Period (2002-2004).

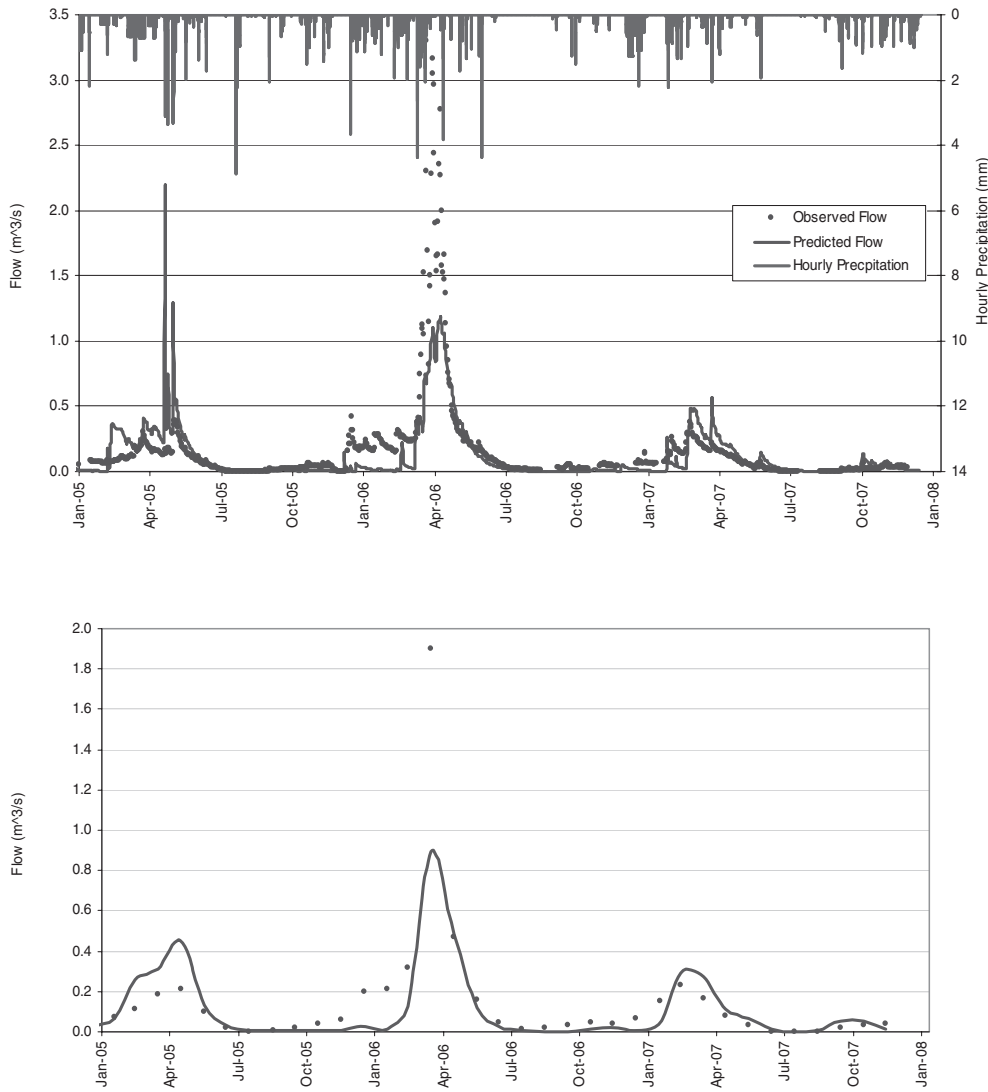


FIGURE 5. Plot of Daily Precipitation With SWAT Simulated and Measured Daily and Monthly Streamflow at Basin Outlet Stream Gage of DCEW for the Validation Time Period (2005-2007).

of these plots indicates that the model predicted streamflow timing and volume well, with the exception of two overpredictions in May and June 2004. In this event the model predicted a strong response to a rain event that was actually negligible. The model performance is summarized in Table 5 through the following summary statistics described earlier: NSE, Dv, VE, RMSE, and R^2 . For the calibration period,

the daily NSE coefficient was optimized, through auto-calibration, to a value of 0.66 with a Dv of -12.9% and R^2 of 0.83. These statistical indicators suggested that the model estimates were satisfactory with only a limited deviation in the estimated streamflow volume and a good fit of the model to the observed streamflow at this daily time step. Motovilov *et al.* (1999) have classified NSE values and propose that values between

TABLE 5. Summary of Statistical Evaluation of SWAT DCEW Model Performance in Predicting Stream and Soil Moisture.

Time Period	Observation	Time Step	NSE	Dv (%)	Ve	RMSE	R^2
2001-2004	Streamflow	Daily	0.66	-12.9	0.57	0.13	0.83
2001-2004	Streamflow	Monthly	0.79	-13.1	0.63	0.08	0.90
2005-2007	Streamflow	Daily	0.54	-20.3	0.54	0.23	0.76
2005-2007	Streamflow	Monthly	0.64	-22.8	0.42	0.19	0.85
February-May (05, 06, 07)	Spring runoff streamflow	Monthly	0.63	-0.19	0.45	0.32	0.84
June-January (05, 06, 07)	Base-flow streamflow	Monthly	0.83	-0.38	0.31	0.05	0.50

NS = 0.36 and 0.75 are “satisfactory.” However, care should be given in applying and interpreting the R^2 statistic for the daily streamflow analysis because over the course of a year it tends to violate the assumptions of normality (Coffey *et al.*, 2004). However, for monthly data any statistical analysis including R^2 is appropriate. The monthly NSE of calibrated streamflow predictions for the calibration time period is 0.79 with a Dv of -13.1% and R^2 of 0.90. These monthly statistics show marked improvement over daily calibrated output with an increased NSE and R^2 , but Dv remained about the same as that of the daily calibration analysis. Others report similar calibration-phase statistics for SWAT model performance in mountain watersheds. For example, Fontaine *et al.* (2002) reported a monthly NSE of 0.86 with a Dv of -9.8% , Lemonds and McCray (2007) reported a monthly NSE of 0.71 (at their most downstream stream gage), and Zhang *et al.* (2008) reported a maximum monthly NSE value of 0.85 and R^2 of 0.87.

As the next step, the model parameters were then set to the calibrated values and the model was validated for the time period of January 2005 through December 2007. To evaluate SWAT’s streamflow predictive ability across a variety of scales, the model-predicted streamflows were compared with observed values from stream gages at the subbasin outlets for the validation time period (2005-2007). In general, a gradual decline was observed in model efficiency (NSE) as the subbasin area decreased (Table 4). For validation purposes the model was allowed to “spin up” for four years before the validation phase from January 2001 through December 2005 using the weather drivers from the calibration period. Figure 5 shows the three-year hydrologic simulation for streamflow at the DCEW outlet gage using the calibrated model over the validation time period. The summary statistics (Table 5) for the validation phase (2005-2007) at the monthly time step were: NSE of 0.64, Dv of -22.8% , RMSE of $0.19 \text{ m}^3/\text{s}$, and R^2 of

0.85. The summary statistics for the validation time period are slightly poorer than those of the calibration-phase because the model does not accurately predict the peak spring runoff of 2006 (Figure 6). Further, the model overpredicts snowmelt flow in April 2005. At the monthly time-step, the model yielded an NSE value of 0.64 while predicting stream discharges at the outlet stream gage of the DCEW. Base flows were better captured (NSE = 0.83) than spring peak runoff flows (NSE = 0.63) with respect to overall model efficiency as measured by the NSE (Table 5). The monthly time step, during the validation phase, again showed better overall model performance than the daily time step, but the daily time step better captured the total volume of runoff. Daily time step statistics show less accuracy through a lower NSE of 0.54, a higher RMSE of $0.23 \text{ m}^3/\text{s}$, and a lower R^2 of 0.76. However, both volumetric metrics show better performance at the daily time step with a slightly lower magnitude Dv of -20.3% and a slightly higher Ve of 0.54.

Soil Moisture

Soil moisture was evaluated temporally at both the point and basin scale using data from the BFL and BFU soil moisture monitoring pits. Since the model was able to capture the trends in streamflow timing and volume at the basin outlet, as quantified by the NSE and Dv metrics, the model predictions were extended to the other water balance components including soil moisture and ET. Figure 6 shows the average observed soil moisture for BFL and BFU sites, in mm of water stored in the entire soil column, and the SWAT-predicted basin-wide average soil moisture contents to an average total soil depth of 1.2 m. The observed maximum and minimum soil moisture for the three years (2005-2007) were approximately 175 mm and 50 mm, respectively, while the model-predicted maximum and minimum values were approximately 125 mm and 25 mm, respectively. The average of the measurements at the BFL and BFU sites provide a surrogate for more extensive data since these two sites are located in different ecosystems at different elevations in the watershed. As mentioned earlier, BFL is located below tree line at an elevation of 1,151 m while BFU is located near tree line elevation, 1,612 m. Figure 6 shows that SWAT captured the timing of both the fall season wetting up of the soil, as well as the early summer drying down of the soil column, as evidenced by the temporal match between predictions and observations. But there was a consistent underprediction of soil moisture in the soil column of approximately 50 mm. It should be noted, however, that the model

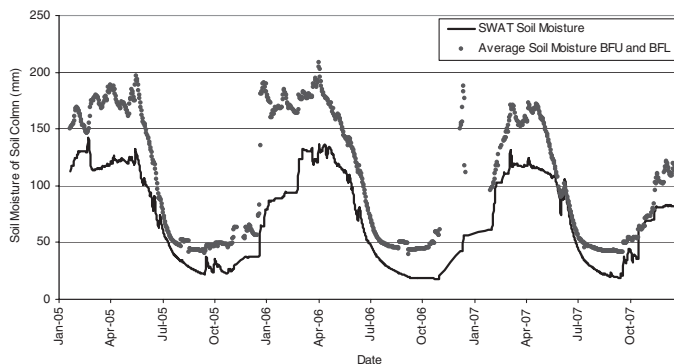


FIGURE 6. Plot of DCEW Basin-Wide Soil Moisture Observations Averaged for BFU and BFL and SWAT Model Predictions for Basin-Wide Soil Moisture for the Entire Soil Column.

is predicting the average soil moisture for an entire HRU (0.03 km²) while measurements were made at specific points. Furthermore, soil moisture observations were made up to 100 cm depths, however, the model might be calculating water content for more than 100 cm for some of the HRUs. Therefore, it could have likely attributed to under/over estimation of soil moisture.

Simulated Water Balance Components

The predicted monthly average values of water balance components were analyzed to investigate the ability of SWAT to partition the incoming precipitation through the hydrologic pathways of soil moisture storage streamflow, ET, and drainage to the deep aquifer from the lowest layer of soil in the soil column. Figure 7 shows the model-predicted monthly hydrologic balance components for each year in the validation period (2005-2007) along with the observed change in soil moisture storage averaged for the BFL and BFU soil moisture monitoring pits (all units are mm). This plot of the components of the hydrologic balance exhibits the monthly response of the model outputs as they are driven by the seasonal atmospheric conditions described by the weather data. As expected, these timing trends corresponded with the general observed trend in the DCEW. Most notably, ET began to rise from near zero values in the winter, to a peak value of approximately 100 mm as the spring snowmelt began to contribute to streamflow and the cool season grasses began to respire in

March. Then the plant activity, as well as evaporation, both dependent on soil moisture, became limited because soil moisture was continually decreased to a value of approximately 25 mm at the beginning of July. However, the mixed coniferous forests of the higher elevations likely continued to transpire by extracting water from deeper soil layers, while the basin-wide soil moisture was at the wilting point of about 50 mm, during this period as suggested by the stable ET values towards the end of the growing season (July through September). The high runoff of spring 2006 showed the highest drainage value of nearly 250 mm while the other two years of the simulation (2005 and 2007) had maximum drainage values of about 75 mm. Drainage began in the spring, peaked with the streamflow during the spring runoff, and then receded with falling soil moisture and streamflow.

Spatial Distribution of SWAT Modeled Soil Moisture and Evapotranspiration

The watershed-scale simulated soil moisture is presented in this section, building on the verification of the model for its prediction of streamflow and soil moisture as described previously. Earlier, more rapid, drying of the BFL site soil moisture each year was observed. Predicted soil moisture and ET over the growing season validation period generally followed the expected trends across the watershed, with lower elevation soils drying more rapidly than higher elevation soils.

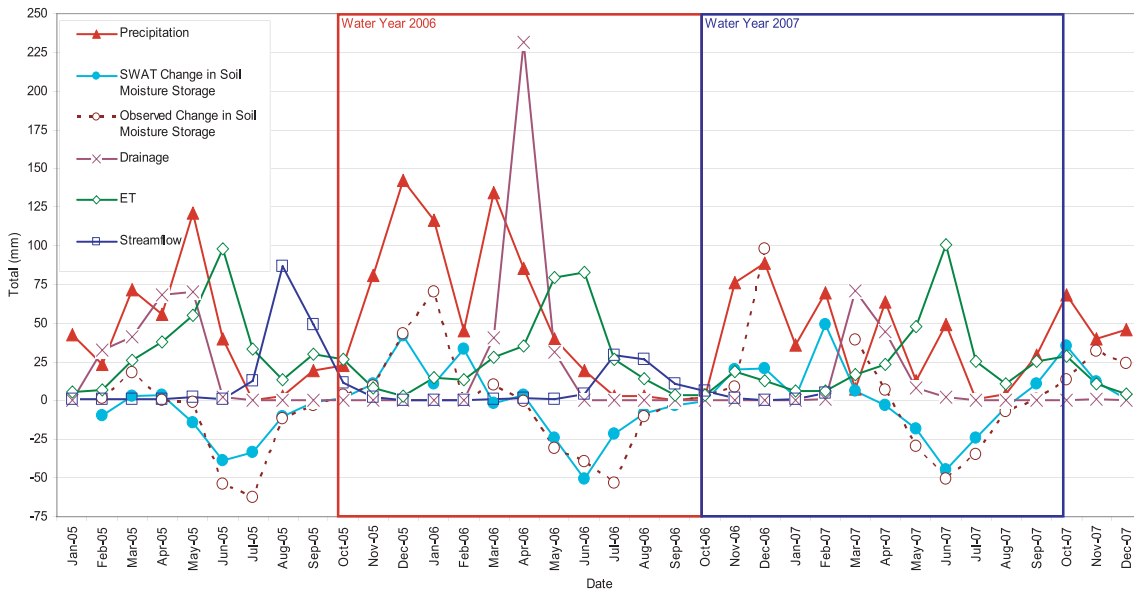


FIGURE 7. Plot of Monthly Hydrologic Budget in mm for the DCEW Showing Total Precipitation, Model Predicted Change in Soil Moisture Storage, Average Change in Soil Moisture Storage Observed at BFU and BFL, Drainage, Evapotranspiration (ET), and Streamflow.

The spatial distribution of SWAT modeled soil moisture and ET (both in mm) over the growing season of 2007 as monthly averages at the HRU scale are shown in Figure 8. These maps demonstrate the distributed model output over the 839 discretized HRUs that are classified through similar soil, vegetation, and land slopes. In Figure 8, soil moistures

ranged from 38 to 336 mm with an average of 138 mm and standard deviation 71 mm for the wet-test period of the season (April). In June, the basin's soil moisture was generally drier but still showed a significant amount of spatial variability with a range of 1-253 mm, an average of 74 mm, and a standard deviation of 61 mm. At the end of the growing season

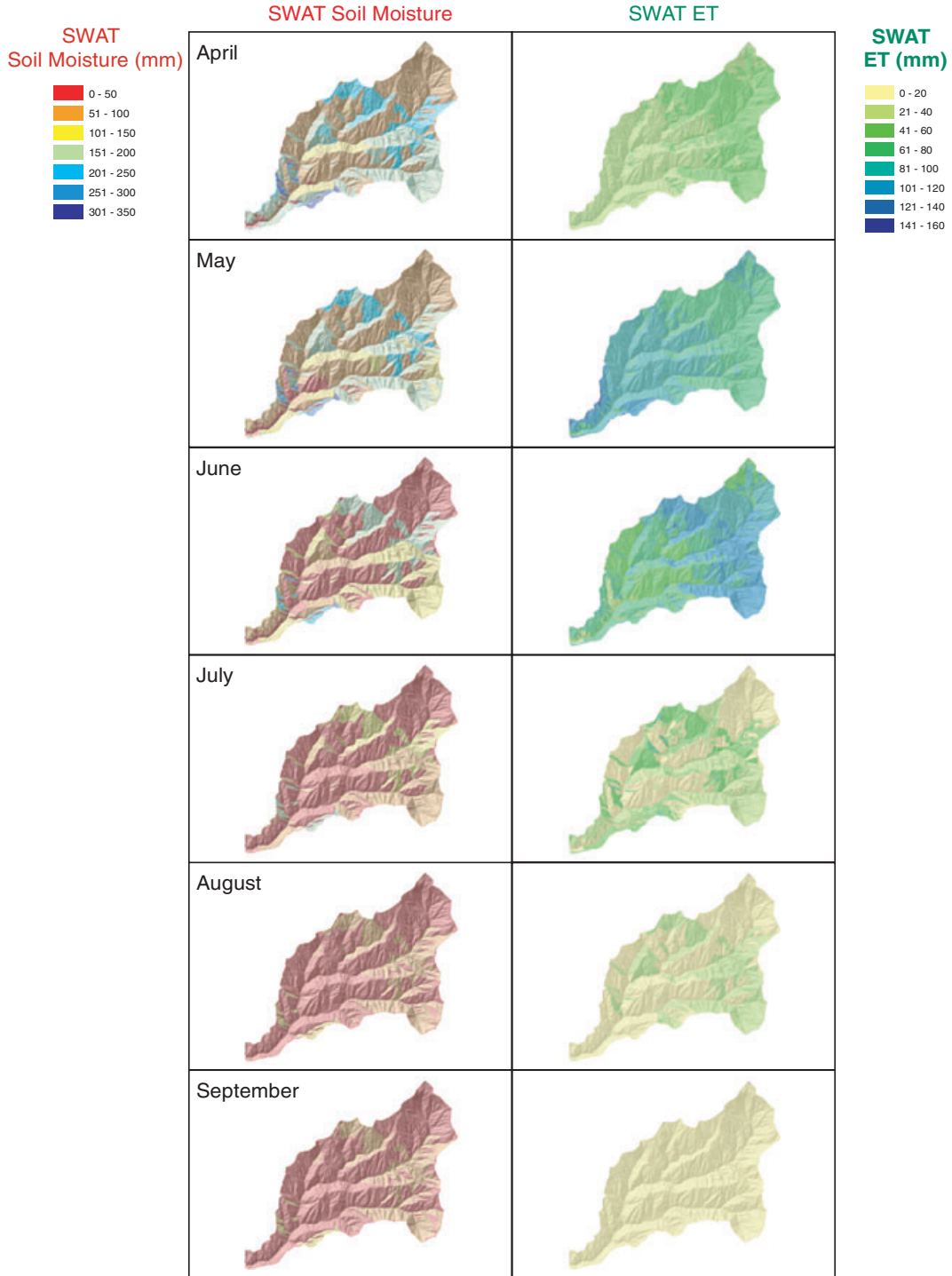


FIGURE 8. Maps Showing Monthly Average SWAT Predicted Soil Moisture and ET (both in mm). Values were distributed over appropriate HRUs.

in September, soil moisture was at its lowest model-predicted value with the least spatial variability: soil moisture ranged from 0 to 134 mm, with an average of 19 mm, and a standard deviation of 29 mm. In general, the model predicted that the lower elevation south facing hillslopes had lower ET and soil moisture values, with moisture dropping to values in the 0-50 mm range by June, while the higher and north-facing elevations retained moisture, retaining 51-100 mm of moisture even as late as September. This elevated soil moisture throughout the growing season on higher elevation north facing slopes supplied moisture to support larger ET values. Higher north facing slopes had ET values in the 21-40 mm range that prevailed as late as August. The soil moisture maps show the lower basin drying earlier in the growing season with values as low as the 0-50 mm range in April. This drying trend propagated to the higher elevations as the growing season moved into the summer months, with much of the upper basin being in the 0-50 mm soil moisture range by June. Again, these drier conditions predominated, as expected, on the south facing slopes. SWAT predicted soil moisture persisting on the north facing slopes through the entire summer as evidenced in the wetter north facing slopes in August and September (Figure 8).

Spatial trends of ET predicted by SWAT matched expectations for seasonal timing and elevation distribution in a manner similar to the soil moisture predictions. ET in April was the highest at the higher elevations where the evergreen vegetation generally dominates the landscape. In May, the vegetation at lower elevations dominated by grasses began to “turn on” and transpire while the vegetation at upper elevations lagged temporarily, with ET values ranging from 61 to 160 mm at lower elevations, and 80-120 mm range in the upper basin. In June and July, the vegetation above the tree line started to contribute the larger portion of the basin’s total ET as the lower elevation grasses senesced in response to the decreased soil moisture in the drying lower basin. Again, the persistence of moisture on the north aspects was evidenced by the persistence of higher ET values into July and August in the range of 41-80 mm while the ET on most of the south facing slopes was in the 0-20 mm range.

DISCUSSION

Streamflow

Daily and monthly predictions of streamflow by SWAT compared well with streamflow measured at

the basin outlet stream gage for the three-year validation period, 2005-2007, with the exception of isolated overpredictions of melt events in the spring of 2005, and underpredictions in spring 2006 (Figure 6). Runoff generation in hillslope-dominated watersheds is controlled in part by the definition of a watershed’s streamflow and flow accumulation network. This drainage system is defined in SWAT by a threshold area for the existence of channelized flow. While the size of the flow accumulation area in this study was set at a value of 0.02 km² after a careful analysis, based on the size of a small subwatershed within the DCEW that has a gaged channelized intermittent stream draining it, an improper selection of flow accumulation area can cause discrepancy in simulating streamflow timing and volume.

Snowmelt Processes

The inclusion of observed precipitation and temperature lapse rates distributed through 100-m elevation bands allowed the model to capture the expected timing and magnitude of both the winter accumulation of snow as shown in Figure 2, as well as the seasonal timing of runoff and soil moisture (Figures 4 and 5). Figure 2 shows a slight dominance of snow over rain (53% snow to 47% rain) for the seven-year modeling period. The timing of accumulated snowmelt appeared to superimpose precisely with the peak observed streamflow in the spring as seen from both calibration and validation periods in Figures 4 and 5, respectively.

SWAT had difficulty capturing the peak runoff during April 2006 in the validation period (Figure 5), which was produced by ROS events. Problems can be attributed to uncertainty in the data to drive SWAT, particularly in the spatial and temporal coverage of precipitation and temperature, but most importantly, the model is not an event-based model and therefore it cannot capture this subdaily dynamics more accurately. Adequate modeling of ROS events requires consideration of the transience of freezing levels as well as the distribution of SWE throughout a basin (McCabe *et al.*, 2007). Also, the variables defining the subdaily snowmelt processes including the intensity and the spatial extent of rain and the accumulated snow on the ground were not available from our measurements nor provided by the model at this spatial and temporal scale.

Since SWAT is a daily simulation model, it relies on a temperature day snowmelt method that might be capturing the snowmelt dynamics over the daily time step but not at the subdaily scale. While this error also draws attention to the fact that high spatial resolution precipitation and temperature data could improve the default methods implemented in SWAT, temperate

index snowmelt methods do not account for energy added to the snowpack by rain to cause enhanced melt. Also, Marks *et al.* (1998) showed that enhanced turbulent energy exchanges during ROS events are more significant than the energy added to the snowpack by rain. However, Zhang *et al.* (2008) investigated the performance of three different snowmelt algorithms on the Yellow River Basin, and concluded that the simple temperature index default method of SWAT performed well as compared with more complex energy balance methods. Zhang *et al.*'s (2008) work, however, was conducted at a much larger scale and did not directly explore the role of ROS events.

Soil Available Water Content

The soil available water content (SOL_AWC) parameter (defined as the difference between field capacity (FC) and wilting point water contents) prescribed in the study provided insight into the function of the overall water balance of the DCEW but required further refinement to contain the model uncertainty. SWAT performed satisfactorily at estimating the timing and seasonality of basin-wide soil moisture (Figure 6, Table 5). However, 25-mm underpredictions of moisture content in the summer dry season and 50-mm underpredictions in the winter wet season soil moisture were observed during the validation period. These offsets could also be attributed to the lack of resolution wherein the model provided areal estimates were compared against the limited point observations, especially from only two points. In addition, the accuracy in the model's initial SSURGO database values for soil obtained for each soil layer could be a suspect as the wilting point (WP) was calculated using these values within the model as a function of clay content and bulk density. Consequently, the FC of the soil layers are calculated by SWAT as the sum of the WP and SOL_AWC will be inaccurate if SOL_AWC and WP were not accurate, thus causing uncertainty in the soil moisture estimates. The maximum and minimum soil moisture values within the SWAT model routines that route water through the soil column are constrained by the values of FC and WP for each soil type. When additional field observations of soil hydraulic conductivity, soil moisture, subsurface flow, and recharge is available, the drainage and soil water availability parameters such as SOL_AWC and RCHRG_DP can further be refined.

Weather Driver Uncertainty

The weather data for this work were collected at two weather stations that have experienced signifi-

cant data interruptions. The gap-filled data were only an estimation of actual weather conditions. Quality-checked, higher spatial resolution precipitation and temperature dataset alone would help to limit the model's uncertainty significantly since there is a high level of spatial variability in the DCEW precipitation pattern and wintertime inversions in the study area.

Another consideration with respect to weather driver precipitation data is the method by which wintertime precipitation data was collected. The weather stations of the DCEW rely on Belfort Universal Rain Gages Series 5-780/5915 (Belfort Instruments, Baltimore, Maryland) to capture snow quantity. This method can result in notable undercatch of snow quantity, especially during precipitation events that occur with wind greater than 2 m/s (Fassnacht, 2004). These errors could be corrected for future work by using a wind correction of the shielded gage values (Yang *et al.*, 1999). Current studies are being conducted to assess the impact of these potential errors. Considering these sources of uncertainty in the parameter estimates and weather drivers, and the simplifications needed for the interpolation of the weather data and necessary model assumptions, the calibrated SWAT model captured general trends of the DCEW streamflow regime.

Vegetation and Soil Moisture Parameterization Effects. ET processes deplete soil moisture by evaporation from the soil surface and by transpiration through plant water uptake from the root zone depth. As discussed earlier, multiple vegetation types were aggregated to one category to be able to remap with that of the model vegetation classes. For instance, ponderosa pine, grand fir, subalpine fir, Douglas fir, and mixed subalpine fir were all combined into one forest type (FRSE). Each of the above forest types has distinct canopy characteristics, and if improvements in predicting how water is attenuated by them are to be made, they should first be treated individually. Otherwise, refinements that may be appropriate for one type may erode grains by inappropriately changing another type. For example, ponderosa pine tends to have more open canopies than subalpine fir. While increasing LAI values, for instance, may improve description of fir, realistic descriptions of pine may be compromised by such global increase (and vice versa). The calibrated EPCO and soil evaporation compensation factor (ESCO) control the shape of the moisture availability curve of the soil column to meet the transpiration and evaporation demands by effectively increasing or decreasing the moisture availability from deeper layers. The autocalibrated unitless EPCO and ESCO parameters values were 0.57 and

0.61, respectively (Table 4). Both EPCO and ESCO vary in value from 0.01 to 1 but their values affect soil moisture availability in opposite ways. For instance, an ESCO value of 1 limits moisture availability for soil evaporation to the top 100 mm while an EPCO value of 1 allows soil moisture extraction availability for transpiration from deeper layers. Reflecting on the underestimated soil moisture results (Figure 7), these mid-range calibrated values appeared to release soil moisture from deeper layers more readily than required for both soil evaporation and plant transpiration.

In addition to direct soil evaporation and plant transpiration, precipitation intercepted by the canopy of the land cover can also play a significant role in the soil moisture balance during the growing season for semiarid watersheds such as the DCEW. Most of the precipitation in the DCEW occurs in the form of winter snowfall but canopy interception of summer precipitation can prevent it from entering the soil column. Because of this importance of the canopy storage during the growing season, two parameters controlling canopy interception were auto-calibrated: maximum leaf area index (BLAI) that varies from 1 to 6 (unitless), and maximum canopy storage (CANMX) that varies from 0 to 10 mm. The calibrated values of these parameters, BLAI and CANMX (Table 5) suggest that the vegetation, at the peak of the growing season, covered 72% of the land and the canopy could intercept up to 8.62 mm of precipitation. Although these high values likely arise as artifacts of calibration, they illustrate the potential impact that vegetation can have on the water balance. Very light summer rainfall that is intercepted can evaporate from vegetation surfaces, and the remaining rain that reaches the ground surface commonly evaporates from shallow soils. Canopy interception can therefore be playing a part in the underprediction of growing season soil moisture since it can reduce the amount of precipitation reaching the soil surface.

It is worth noting that SWAT was calibrated to an objective function based on streamflow measurements alone. Integration of soil moisture prediction performance into the calibration procedures could greatly improve the model's predictive abilities. Use of multiple objective functions including nutrient and sediment loads is possible with the ArcSWAT GUI, but currently, inclusion of soil moisture data is not an option. This study showed the model was capable of capturing the general trend of the basin wide soil moisture without calibration to soil moisture, but the model performance could be improved to better capture the quantity of water stored in the soil column, and the layer-wise distribution of the volume of water throughout the soil.

CONCLUSIONS

The SWAT hydrologic model was applied to the semiarid DCEW to investigate the water balance components of the watershed both temporally and spatially and it performed well at predicting basin outlet streamflow with a NSE of 0.79 and Dv of -13.1% for monthly predictions. SWAT adequately captured both the spring peak flows and the summer base flows during the calibration phase, nonetheless, soil moisture was generally underestimated compared with observations from two monitoring pits. (Note: comparisons were made between point measurements and HRU-scale estimates.) This underestimation indicates that further refinement of the watershed's soil properties and improved representation of subsurface flow mechanics and snow processes with additional field observations to refine the key parameters pertaining to soil (e.g., available water content and saturated hydraulic conductivity), snow (e.g., lapse rates, melting), and vegetation (e.g., leaf area index and maximum canopy index) is crucial for better prediction of soil moisture and streamflow. However, these parameters are not well-known due to limitations in the availability of field-measured values and improved representation of flow mechanics generally comes at the expense of computational efficiency.

Monthly hydrologic budget estimates by SWAT for the three-year calibration phase appropriately accounted for the timing and relative magnitude of ET and soil moisture. The spatio-temporal distribution of these components during the growing season of 2007 agreed with the expected effects of elevation and aspect with the timing of these processes, with higher soil moistures persisting at the higher elevations and on north facing slopes, and temporal variation of soil moisture affecting ET. Investigation of the accuracy of these model outputs was limited to measured soil moisture and streamflow for quantitative evaluation at selected locations.

The variability in snow accumulation and melt and its impact on water balance components, especially soil moisture, emphasizes the important role of the parameterization of the lapse rates through high density precipitation and temperature datasets. The temperature lapse rate, in particular, is difficult to quantify meaningfully for the DCEW because of frequent wintertime inversions in which the lapse rate shows an increase in temperature. These inversions are the result of a stable cold air mass near the surface being confined by a high-pressure system and/or upper level warmer conditions. This positive temperature lapse rate is not accounted for by the overall yearly average negative rate, making it difficult for proper distribution of the predominantly wintertime

precipitation. Successful evaluation of SWAT in semi-arid mountainous watersheds as illustrated in this investigation to compute the water balance components can provide unique opportunity of extending the model to other ungaged basins in the region.

ACKNOWLEDGMENTS

This research was supported in part by the NSF-Idaho EPSCoR Program and the National Science Foundation under award number EPS-0447689 and EPS-0814387.

LITERATURE CITED

- Abbaspour, K.C., J. Yang, I. Maximov, R. Siber, K. Bogner, J. Mieleitner, J. Zobrist, and R. Srinivasan, 2007. Modeling Hydrology and Water Quality in the Pre-Alpine/Alpine Thur Watershed Using SWAT. *Journal of Hydrology* 333(2-4):413-430.
- Ahl, R.S., S.W. Woods, and H.R. Zuuring, 2008. Hydrologic Calibration and Validation of SWAT in a Snow-Dominated Rocky Mountain Watershed, Montana. *Journal of the American Water Resources Association* 44(4):1-21.
- Aishlin, P., 2006. Groundwater Recharge Estimation Using Chloride Mass Balance, Dry Creek Experimental Watershed. Masters Thesis, Department of Geosciences, Boise State University, Boise, Idaho.
- Arnold, J.G. and N. Fohrer, 2005. SWAT2000: Current Capabilities and Research Opportunities in Applied Watershed Modeling. *Hydrological Processes* 19(3):563-572.
- Arnold, J.G., R. Srinivasan, R.S. Muttiah, and J.R. Williams, 1998. Large Area Hydrologic Modeling and Assessment Part I: Model Development. *Journal of American Water Resources Association* 34(1):73-89.
- ASCE (American Society of Civil Engineers Task Committee on Definition of Criteria for Evaluation of Watershed Models of the Watershed Management Committee, Irrigation, and Drainage Division), 1993. Criteria for Evaluation of Watershed Models. *Journal of Irrigation and Drainage Engineering* 119(3) 429-442.
- Bales, R.C., N.P. Molotch, T.H. Painter, M.D. Dettinger, R. Rice, and J. Dozier, 2006. Mountain Hydrology of the Western United States. *Water Resources Research* 42(7), W08432, doi:10.1029/2005WR004387.
- Caicco, S.I., J.M. Scott, B. Butterfield, and B. Csuti, 1995. A GAP Analysis of the Management Status of the Vegetation of Idaho (U.S.A.). *Conservation Biology* 9(3):498-511.
- Chandler, D.G., M. Seyfried, M. Murdock, and J.P. McNamara, 2004. Field Calibration of Water Content Reflectometers. *Soil Science Society of America Journal* 68(5):1501-1507.
- Coffey, M.E., S.R. Workman, J.L. Taraba, and A.W. Fogle, 2004. Statistical Procedures for Evaluating Daily and Monthly Hydrologic Model Predictions. *Transactions of ASAE* 47(1):59-68.
- Criss, R.E. and W.E. Winston, 2008. Do Nash Values Have Value? Discussion and Alternate Proposals *Hydrological Processes* 22(14):2723-2729.
- Duan, Q., S. Sorooshian, and V. Gupta, 1992. Effective and Efficient Global Optimization for Conceptual Rainfall-Runoff Models. *Water Resources Research* 28(4):1015-1031.
- Duan, Q., S. Sorooshian, and V. Gupta, 1994. Optimal Use of the SCE-UA Global Optimization Method for Calibrating Watershed Models. *Journal of Hydrology* 158(3-4):265-284.
- Eckhardt, K., S. Haverkamp, N. Fohrer, and H.-G. Frede, 2002. SWAT-G, a Version of SWAT99.2 Modified for Application to Low Mountain Range Catchments. *Physics and Chemistry of the Earth* 27(9-10):641-644.
- Entin, J., A. Robock, K.Y. Vinnikov, V. Zabelin, S. Liu, A. Namkhai, and T. Adyasuren, 1999. Evaluation of Global Soil Wetness Project Soil Moisture Simulations. *Journal of the Meteorological Society of Japan* 77(1B):183-198.
- Fassnacht, S.R., 2004. Estimating Alter-Shielded Gauge Snowfall Undercatch, Snowpack Sublimation, and Blowing Snow Transport at Six Sites in the Conterminous USA. *Hydrologic Processes* 18(18):3481-3492.
- Flerchinger, G.N., C.L. Hanson, and J.R. Wight, 1996. Modeling Evapotranspiration and Surface Energy Budgets Across a Watershed. *Water Resources Research* 32(8):2539-2548.
- Fohrer, N., S. Haverkamp, and H.G. Frede, 2005. Assessment of the Effects of Land Use Patterns on Hydrologic Landscape Functions: Development of Sustainable Land Use Concepts for Low Mountain Range Areas. *Hydrological Processes* 19(3):659-672.
- Fontaine, T.A., T.S. Cruickshank, J.G. Arnold, and R.H. Hotchkiss, 2002. Development of a Snowfall-Snowmelt Routine for Mountainous Terrain for the Soil Water Assessment Tool (SWAT). *Journal of Hydrology* 262(1-4):209-223.
- Garen, D.C. and D.S. Moore, 2005. Curve Number Hydrology in Water Quality Modeling: Uses, Abuses, and Future Direction. *Journal of American Water Resources Association* 41(2):377-388.
- Gassman, P.W., M.R. Reyes, C.H. Green, and J.G. Arnold, 2007. The Soil and Water Assessment Tool: Historical Development and Future Research Directions. *Transactions of the American Society of Agricultural and Biological Engineers* 50(4):1211-1250.
- Grant, L., M. Seyfried, and J. McNamara, 2004. Spatial Variation and Temporal Stability of Soil Water in a Snow-Dominated, Mountain Catchment. *Hydrological Processes* 18(18):3493-3511.
- Green, W.H. and G.A. Ampt, 1911. Studies on Soil Physics, 1 The Flow of Air and Water Through Soils. *Journal of Agricultural Sciences* 4:11-24.
- Gribb, M.M., I. Forkutsa, A. Hansen, D. Chandler, and J. McNamara, 2009. The Effect of Various Soil Hydraulic Property Estimates on Soil Moisture Simulations. *Vadose Zone Journal* 8(2):321-331, doi:10.2136/vzj2008.0088.
- Hernandez, M., S.N. Miller, D.C. Goodrich, B.F. Goff, W.G. Kepner, C.M. Edmonds, and K.B. Jones, 2000. Modeling Runoff Response to Land Cover and Rainfall Spatial Variability in Semi-Arid Watersheds. *Environmental Monitoring and Assessment* 64(1):285-298. DOI 10.1023/A:1006445811859.
- Houser, P.R., W.J. Shuttleworth, J.S. Famiglietti, H.V. Gupta, K.H. Syed, and D.C. Goodrich, 1998. Integration of Soil Moisture Remote Sensing and Hydrologic Modeling Using Data Assimilation. *Water Resources Research* 34(12):3405-3420.
- Huang, J., M. Hugg, H.M. van den Dool, and K.P. Georgarakos, 1996. Analysis of Model-Calculated Soil Moisture over the United States (1931-1993) and Applications to Long-Range Temperature Forecasts. *Journal of Climate* 9:1350-1362.
- Idaho Geospatial Data Clearinghouse, 2004. Digital Elevation of Tile 07, Idaho With a Horizontal Grid Spacing of 10-Meters. Idaho Geospatial Data Clearinghouse, Moscow, Idaho. http://data.insideidaho.org/data/IGDC/archive/elev10m/elev10m_tile07_igdc.tgz, accessed July 14, 2007.
- Jayakrishnan, R., R. Srinivasan, C. Santhi, and J.G. Arnold, 2005. Advances in the Application of the SWAT Model for Water Resources Management. *Hydrological Processes* 19(3):749-762.
- Landscape Dynamics Lab, 1999. Land Cover of Idaho: Idaho Cooperative Fish and Wildlife Research Unit, Moscow, Idaho. http://data.insideidaho.org/data/icfwru/archive/landcov_id_icfwru.zip, accessed July 14, 2007.

- Lemons, P.J. and J.E. McCray, 2007. Modeling Hydrology in a Small Rocky Mountain Watershed Serving Large Urban Populations. *Journal of Water Resources* 43(4):1-13.
- Li, J. and S. Islam, 2002. Estimation of Root Zone Soil Moisture and Surface Fluxes Partitioning Using Near Surface Soil Moisture Measurements. *Journal of Hydrology* 259(1-2):1-14.
- Marks, D., J. Kimball, D. Tingey, and T. Link, 1998. The Sensitivity of Snowmelt Processes to Climate Conditions and Forest Cover During Rain-on-Snow: A Case Study of the 1996 Pacific Northwest Flood. *Hydrologic Processes* 12(10-11):1569-1587.
- McCabe, J.G., M.P. Clark, and L.E. Hay, 2007. Rain-on-Snow Events in the Western United States. *Bulletin American Meteorological Society* 88(3):319-328.
- McCuen, R.H., Z. Knight, and A.G. Cutter, 2006. Evaluation of the Nash-Sutcliffe Efficiency Index. *Journal of Hydrologic Engineering ASCE* 11(6):597-602.
- McNamara, J.P., D. Chandler, M. Seyfried, and S. Achet, 2005. Soil Moisture States, Lateral Flow, and Streamflow Generation in a Semi-Arid, Snowmelt-Driven Catchment. *Hydrologic Processes* 19(20):4023-4038.
- Mein, R.G. and C.L. Larson, 1973. Modeling Infiltration During a Steady Rain. *Water Resources Research* 9(2):384-394.
- Mote, P.W., E.A. Parson, A.F. Hamlet, W.S. Keeton, D. Lettenmaier, N. Mantua, E.L. Miles, D.W. Peterson, D.L. Peterson, R. Slaughter, and A.K. Snover, 2003. Preparing for Climatic Change: The Water, Salmon, and Forests of the Pacific Northwest. *Climatic Change* 61(1-2):45-88.
- Motovilov, Y.G., L. Gottschalk, K. Engeland, and A. Rodhe, 1999. Validation of a Distributed Hydrological Model Against Spatial Observations. *Agricultural and Forest Meteorology* 98-99:257-277.
- Narasimhan, B., R. Srinivasan, J.G. Arnold, and M. Di Luzio, 2005. Estimation of Long-Term Soil Moisture Using a Distributed Parameter Hydrologic Model and Verification Using Remotely Sensed Data. *Transactions of Agricultural Engineers* 48(3):1101-1113.
- Nash, J.E. and J.V. Sutcliffe, 1970. River Forecasting Through Conceptual Models Part I – A Discussion of Principles. *Journal of Hydrology* 10(3):282-290.
- Natural Resources Conservation Service, United States Department of Agriculture, 2005. Soil Survey Geographic (SSURGO) Database for Ada and Boise County, Idaho. <http://soildatamart.nrcs.usda.gov>, accessed September 21, 2007.
- Natural Resources Conservation Service, United States Department of Agriculture, 2006. U.S. General Soil Map (STATSGO2) for Idaho. <http://soildatamart.nrcs.usda.gov>, accessed September 21, 2007.
- Nayak, A., D.G. Chandler, D. Marks, J.P. McNamara, and M. Seyfried, 2008. Correction of Electronic Weighing Bucket Precipitation Gauge Measurements. *Water Resources Research*, 44:W00D11, doi:10.1029/2008WR006875.
- Neitsch, S.L., J.G. Arnold, J.R. Kiniry, and J.R. Williams, 2005. Soil and Water Assessment Tool, Theoretical Documentation, Version 2005, Grassland, Soil and Water Research Laboratory, Temple, TX, Blackland Research and Extension Center, Temple, Texas, Texas Water Resource Institute, College Station.
- NRCS SNOTEL, 2007. Site Information and Reports for Bogus Basin. <http://www.wcc.nrcs.usda.gov/snotel.pl?sitenum=978&state=id>, accessed October 11, 2007.
- Olivera, F., M. Valenzuela, R. Srinivasan, J. Choi, H. Cho, S. Koka, and A. Agrawal, 2006. ArcGIS-SWAT: A Geodata Model and GIS Interface for SWAT. *Journal of the American Water Resources Association* 42(2):295-309.
- Rudzitis, G. and R. Johnson, 2000. The Impact of Wilderness and Other Wildlands on Local Economies and Regional Development Trends. *USDA Forest Service Proceedings RMRS-P-15(2)*: 14-26.
- Ryu, Y., D. Baldocchi, S. Ma, and T. Hehn, 2008. Interannual Variability of Evapotranspiration and Energy Exchange Over an Annual Grassland in California. *Journal of Geophysical Research* 113:(D09104): doi:10.1029/2007JD009263.
- Santhi, C., J.G. Arnold, J.R. Williams, W.A. Dugas, and L. Hauk, 2001. Validation of the SWAT Model on a Large River Basin With Point and Nonpoint Sources. *Journal of the American Water Resources Association* 37(5):1169-1188.
- Schüttmeyer, D., A.F. Moene, A.M. Holtslag, H.A.R. De Bruin, and N. Van De Giesen, 2006. Surface Fluxes and Characteristics of Drying Semi-Arid Terrain in West Africa. *Boundary Layer Meteorology* 118(3):583-612.
- SCS (Soil Conservation Service), 1972. Section 4: Hydrology in National Engineering Handbook. United States Government Printing Office, Washington, DC.
- Soil Survey Staff, 1975. Soil Taxonomy: A Basic System of Soil Classification for Making and Interpreting Soil Surveys. USDA-SCS Agric. Handbook 436, US Government Printing Office, Washington, DC.
- Sridhar, V., K.G. Hubbard, and D.A. Wedin, 2006. Assessment of Soil Moisture Dynamics of the Nebraska Sandhills Using Long-Term Measurements and a Hydrology Model. *Journal of Irrigation and Drainage Engineering* 132(5):463-473.
- Srinivasan, R., T.S. Ramanarayanan, J.G. Arnold, and S.T. Bednarz, 1998. Large Area Hydrologic Modeling and Assessment Part II: Model Application. *Journal of the American Water Resources Association* 34(1):91-101.
- Sun, G., A. Noormets, J. Chen, and S.G. McNulty, 2008. Evapotranspiration Estimates From Eddy Covariance Towers and Hydrologic Modeling in Managed Forests in Northern Wisconsin, USA. *Agricultural and Forest Meteorology* 148(2): 257-267.
- Sun, H. and P.S. Cornish, 2005. Estimating Shallow Groundwater Recharge in the Headwaters of the Liverpool Plains Using SWAT. *Hydrological Processes* 19(3):795-807.
- van Griensven, A., T. Meixner, S. Grunwald, T. Bishop, M. Diluzio, and R. Srinivasan, 2006. A Global Sensitivity Analysis Tool for the Parameters of Multi-Variable Catchment Models. *Journal of Hydrology* 324(1-4):10-23.
- Wang, X. and A.M. Melesse, 2006. Effects of STATSGO and SSURGO as Inputs on SWAT Model's Snowmelt Simulation. *Journal of the American Water Resources Association* 42(5):1217-1236.
- White, K.L. and I. Chaubey, 2005. Sensitivity Analysis, Calibration, and Validations for a Multisite and Multivariable SWAT Model. *Journal of the American Water Resources Association* 41(5):1077-1089.
- Williams, C.J., J.P. McNamara, and D.G. Chandler, 2008. Controls on the Spatial and Temporal Variation of Soil Moisture in a Mountainous Landscape: The Signatures of Snow and Complex Terrain. *Hydrology and Earth System Science Discussion*, 5:1927-1966.
- Williams, J.R., 1969. Flood Routing With Variable Travel Time of Variable Storage Coefficients. *Transactions of the American Society of Agricultural Engineers* 12(1):100-103.
- Yang, D., B.E. Goodison, J.R. Metcalfe, P. Louie, G. Leavesley, D. Emerson, C.L. Hanson, V.S. Golubev, E. Elomaa, T. Gunther, T. Pangburn, E. Kang, and J. Micovik, 1999. Quantification of Precipitation Measurement Discontinuity Induced by Wind Shields on National Gauges. *Water Resources Research* 35(2):491-508.
- Zhang, X., R. Srinivasan, B. Debele, and F. Hao, 2008. Runoff Simulation of the Headwaters of the Yellow River Using the SWAT Model With Three Snowmelt Algorithms. *Journal of the American Water Resources Association* 44(1):48-61.